Very High Efficiency Porous Silica Layer Open-Tubular Capillary Columns Produced via in-Column Sol−Gel Processing

Hara, Takeshi; Futagami, Shunta; Eeltink, Sebastiaan; De Malsche, Wim; Baron, Gino; Desmet, Gert

Published in:
Analytical Chemistry

DOI:
10.1021/acs.analchem.6b02713

Publication date:
2016

License:
Unspecified

Document Version:
Accepted author manuscript

Very high efficiency porous silica layer open-tubular capillary columns produced via in-column sol-gel processing

Takeshi Hara, Shunta Futagami, Sebastiaan Eeltink, Wim De Malsche, Gino V. Baron, Gert Desmet*

Department of Chemical Engineering, Vrije Universiteit Brussels, Pleinlaan 2, 1050 Brussels, Belgium

*Corresponding author
Tel.: +32 (0) 2 629 3251, Fax.: +32 (0) 2 629 3248, E-mail: gedesmet@vub.ac.be

Abstract

It is demonstrated that 5 micrometer i.d. capillaries can be coated with mesoporous silica layers up to 550 nm thickness. All the columns produced using in-column sol-gel synthesis with tetramethoxysilane provide plate height curves that closely follow the Golay-Aris theory. In 60 cm long columns, efficiencies as high as N = 150,000 and N = 120,000 were obtained for respectively a 300 nm and a 550 nm thick porous layer. An excellent retention and plate height reproducibility was obtained when the recipes were subsequently applied to produce very long (1.9 and 2.5 m) capillaries. These columns produced efficiencies up to N = 600,000 for a retained, and around N = 1,000,000 plates for an unretained component. Given the good reproducibility on the long capillaries, and considering that mesoporous silica is still the preferred support for LC, it is believed the present study could spur a renewed interest in open-tubular LC.

1. Introduction

Despite their intrinsic superiority in terms of speed and efficiency, open-tubular LC (OT-LC) and CEC columns have never come close to the widespread success the open-tubular capillary column format is displaying in GC.[1–8] This is due to the fact that the diffusion occurs roughly 10,000 times slower in liquids than in gases, necessitating the use of very narrow column i.d.'s in LC compared to GC. Ideally, these should be on the order of a few micrometer or even less in LC.[9–10] As a consequence, the mass loadability and detection sensitivity of OT-LC columns does not even come close to that of packed bed HPLC columns, which typically have an i.d. of a few mm. It is only for applications where the sample volume is limited that analysts want to move to smaller column cross-sections, to prevent their samples would be too strongly diluted. This has led to the success of capillary packed bed columns in proteomics and metabolomics studies.[7,11–15] With the growing desire to study ever smaller samples, down to the single cell level, combined with the growing sensitivity of mass spectrometry, it is straightforward to expect that future research in biology and life sciences will want to address samples that are so small that the minimal cross-section of OT-LC columns will become the method of choice, especially given their intrinsic ability to produce very high efficiencies, in turn owed to their very low flow resistance. This trend was recognized a few years ago by Karger's group.[7,16,17]

To overcome their poor mass loadability, and concomitantly poor detection sensitivity, many research efforts have already been made (mainly in the 1980's and 1990's) to increase the retention surface of OT-columns. Besides approaches to roughen the inner wall,[18,19] these efforts can roughly be divided in polymer-based and silica-based wall coatings.

Polymer-based coatings for OT-LC and CEC have been commonly produced using free-radical polymerization techniques with either thermal- or photo-initiation, using a suitable functional monomer and a proper amount of porogen and radical-initiator.[16,20–28] A challenge with these

methods is that they require a very precisely control over the polymerization rate and energy for the heat- or photo-initiation as well as the stoichiometric composition of the polymerizing mixture to ensure that the polymer-based layer only forms on the capillary-wall.[29,30] Despite these difficulties, many different polymer-based coating techniques have been successfully applied to produce PLOT capillary columns. For example, Swart et al. applied in-situ photo polymerization to fabricate polyacrylate stationary phases containing either alkyl or ether group in an i.d. 5 μm capillary, providing over 200,000 plates for retained solutes with the 1.1 m porous layered open tube (PLOT) capillary column.[20] Recently, Collins et al. demonstrated the fabrication of bonded polymer porous layers of polystyrene-divinylbenzene or butyl methacrylate-ethylene dimethacrylate on the walls of fused-silica capillaries via laminar flow thermally-initiated polymerization.[22] A wide range of porous layer thickness was prepared, varying between 50 nm and 25 μm in columns with varying length (30–150 cm) and i.d. (50–200 μm).

The fabrication of silica-based PLOT columns on the other hand was first introduced by Tock et al., using the precipitation of pre-gelled polyethoxysilane prepared from a sol solution containing tetraethoxysilane (TEOS).[31] Since then, several preparation techniques have been applied to enhance the retention and loadability for high resolution separations. In the 1990's, Guo and Colon fabricated silica-based PLOT capillary columns for LC and CEC by using sol-gel processing with a silica precursor mixture of *n*-octyltriethoxysilane (C_8-TEOS) and TEOS,[32–34] resulting in an enhanced retention as well as a high stationary phase stability in both acidic and alkali conditions, which is due to the Si-C bonding from the silica precursor.[32] In 2009, our group used sol-gel processing using spinodal decomposition, the so-called "wetting transition",[35,36] to produce silica porous layers on the surface of the cylindrical pillars in micro-fabricated pillar-array columns.[37–39] Forster et al. recently applied the same sol-gel approach to fabricate PLOT capillary columns with a 10–20 μm i.d. to perform normal-phase LC without surface modification, as well as RPLC after C_8-modificaiton with octyldimethyl-*N*,*N*-dimethylaminosilane.[40–42] In RPLC, it was reported that their C_8-modifed PLOT column with a 15 μm i.d. and a silica porous layer with 500 nm thickness can provide a plate height of H = 18 μm for propylbenzene at a linear velocity (u_0) of 1 mm/s (optimal u_0-value) while providing a 180 times higher column permeability than that of a 100 μm i.d. monolithic silica capillary column.[41]

In the present study, we tried to further reduce the capillary diameter compared to the aforementioned Forster and Altmaier study, as well as to further increase the phase ratio (i.e. the ratio of porous layer thickness to capillary diameter) because it is well known that, for LC applications, relatively thick layers can be afforded before the porous layer thickness starts to really affect the kinetic performance of the columns.[9,10] Three different recipes with increasing tetramethoxysilane (TMOS) content were tested. These recipes were carefully tuned to achieve the right capillary wall wetting transition conditions by optimizing the amount of polyethylene

glycol (PEG) for every different amount of TMOS. This tuning work was carried out in 10 cm capillaries. Subsequently, 60 cm long OT-LC columns were produced with the final recipes and a detailed physical and chromatographic characterization of the produced mesoporous layers was made. Finally, the recipes were applied to produce some very long (2 to 2.5 m) OT-LC columns.

2. Experimental

2.1. Chemicals and materials

Toluene (HPLC grade, > 99.8%), tetramethoxysilane (TMOS), 1 M aqueous acetic acid solution, and polyethylene glycol (PEG) of molecular weight (MW) = 10,000 g/mol were obtained from Sigma-Aldrich Co. (Diegem, Belgium). Octadecyldimethyl-*N*,*N*-dimethylaminosilane was purchased from ChemPur Feinchemikalien und Forschungsbedarf GmbH (Karlsrule, DE). Methanol (HPLC super-gradient grade) was obtained from Biosolve B.V. (Valkenswaard, NL). Deionized water was produced in-house with a Milli-Q water purification system Merck Millipore (Billerica, MA, USA). Coumarin 440 (C440: 7-amino-4-methyl-2*H*-1-benzopyran-2-one), coumarin 450 (C450: 7-(ethylamino)-4,6-dimethyl-2*H*,-1-benzopyran-2-one), coumarin 460 (C460: 7-(diethylamino)-4-methyl-2*H*-1-benzopyran-2-one), and coumarin 480 (C480: 2,3,6,7-tetrahydro-9-methyl-1*H*,5*H*,11*H*-[1]benzopyrano-[6,7,8-ij]quinolizin-11-one) were purchased from Vadeno Optical Solutions (Apeldoorn, NL). Samples were prepared by dissolving these coumarins in the mobile phase to a concentration of 2 mM per component. PTFE filters (0.20 µm × 25 mm) were purchased from Macherey-Nagel (Düren, DE). Fused-silica capillaries with an inner diameter (i.d.) of 5 µm and 10 µm, possessing an outer diameter of 375 µm were purchased from Polymicro Technologies (Phoenix, AZ, USA).

2.2. Preparation of porous layered open tube capillary columns

Porous silica layer in fused-silica capillaries were produced by applying the “wetting transition” effect that can be induced via sol-gel processing.[35–42] Table 1 shows the three sol-gel recipes A, B, and C used in the present study. An example preparation procedure goes as follows: a mixture feed solution was prepared with 7.2 mL TMOS, 0.09 g urea, 10 mL 0.01 M aqueous acetic acid solution, and 0.730 g PEG with MW = 10,000 g/mol, according to a preparation process already described previously to prepare monolithic silica columns.[43] The feed solution was filled in 30 cm PEEK tubing with 700 µm i.d. (IDEX Health & Science GmbH, Erlangen, DE) using a syringe and then the loading loop was connected to a fused-silica capillary with 5 µm i.d. (ca. 80 cm in length). Then, the other side of the PEEK tubing was connected to the PEEK tubing line (250 µm i.d., IDEX Health & Science GmbH) from the HPLC pump filled by 0.01 M aqueous acetic acid solution, which is the loading solvent to push the feed solution into the capillary. The mixture feed solution was charged into the fused-silica capillary under a pressure of 50 bar for 30 min by applying the HPLC pump. After filling, the gelation in the capillary took place at 25 °C for 20 h. The subsequent

processes such as hydrothermal treatment at 95 °C to form mesopores and washing the capillary columns with methanol were executed according to a protocol already described earlier for the production of monolithic silica capillary columns.[44] After the washing process, the fabricated capillary columns were dried at 120 °C in an oven for 24 h.

After the fabrication of the PLOT columns, in-situ functionalization of the bare mesopore surfaces in the silica layers was carried out with 20:80% (*v*/*v*) octadecyldimethyl-*N*,*N*-dimethylaminosilane (ODS-DMA)/toluene mixture solution following a procedure similar to that used previously for the synthesis of monolithic silica capillary columns.[44] In addition, silica-bulk rods were prepared with the same feed compositions shown in Table 1, in order to investigate the mesoporous structures, as demonstrated earlier.[44]

2.3. Measurements

The LC instrument consisted of an LPG-3400M pump (Thermo Fisher Scientific, Germering, DE), a Rheodyne 7125 manual injector with an 5 μL sample loop (IDEX Health & Science GmbH) with home-build T-split injection flow system, a fluorescence microscope IX-71 equipped with the U-RFT-T lamp power supply (Olympus, Tokyo, JP), and a charge-coupled device camera C4742-95-12ERG (Hamamatsu Photonics, Shizuoka, JP). The split ratio was maintained around 1/250,000 for the 5 um i.d PLOT capillary columns during the measurements, to properly realize picoliter injection volumes and nanoliter flow rates (it should be noted that the volume of a 5 μm i.d. capillary is on the order of nanoliters, e.g. 10 nL for a 50 cm long 5 μm i.d. capillary).[4] With an estimated injection volume of about 2 μL (partial loop injection), this 1/250,000 split corresponds to an estimated injection volume of 8 pL. For the on-column fluorescence detection, the excitation wavelength was set at 360–420 nm with a XF1075 387AF28 filter (Omega Optical Inc., VT, USA) and fluorescence wavelength was at 400–500 nm with MF460-80 filter (Thorlabs Elliptec GmbH, Dortmund, DE), respectively. Coumarin compounds were used to carry out column performance tests under the aforementioned measurement conditions using 60:40%–100:0% (*v*/*v*) methanol:water as mobile phase. The fluorescence microscope images were processed with MatLab 2012b software (Mathworks, MA, USA), to visualize the chromatograms.

For the SEM measurements, slices of the PLOT capillary columns were produced with a ceramic cutter, and a thin gold coating was applied using a sputter coater (208 HR, Cressington Scientific instruments Ltd, Watford, UK). SEM images were recorded using a field-emission scanning electron microscope JSM-7100F from JEOL Ltd. (Tokyo, JP). The capillary diameter size and porous-silica layer thickness size were measured from SEM pictures by clockwise rotating a straight line running through the center point of the capillary in steps of 45 degrees, and subsequently averaging the values.

Argon physisorption measurements of the bulk-silica rods were conducted at -186 °C (87 K) to determine the mesopore size distribution, the mesopore volume, and the surface area by applying the non-local density functional theory,[45–47] using an Autosorb-1-MP instrument (Quantachrome corporation, FL, USA).

3. Results and discussion

3.1. Physical characterization

Figs. 1a-c show SEMs of the obtained layers in three 60 cm long, 5 µm i.d. capillaries, respectively coated with recipes A, B, C, essentially differing in the amount of TMOS (see Experimental). From the SEMs, an accurate determination of the layer thickness (δ), the flow-through diameter (d) and the original i.d. of the uncoated capillary ($d_{cap} = d + 2\delta$) could be made (see Fig. 1a for the geometrical definition of d, δ and d_{cap}). The results are reported in Table 2 (average of measurement at 16 different positions). Also reported is the volumetric phase ratio (m), i.e., the ratio of the porous layer volume to that of the flow-through volume:

$$m = \frac{V_{layer}}{V_{flow-through}} = \frac{(d+2\delta)^2 - d^2}{d^2} \quad (1)$$

as well as the external porosity (ε_e), i.e., the fraction of the original uncoated capillary remaining as the flow-through region.

Obviously, the layer thickness and the phase ratio m reported in Table 2 for the experiments in the 5 µm i.d. capillary columns increase with increasing amount of TMOS. The fabricated PLOT columns can provide up to m = 0.55, which is higher than that (m = 0.15) of a 15 µm i.d. PLOT columns with a 500 nm thickness, previously reported by Forster and Altmaier.[41] In an additional experiment, we also applied recipe A in a 10 µm i.d. capillary. In this case, a layer thickness of 560 nm was measured (see supporting information (SI), Fig. S-1), corresponding to a phase ratio m = 0.24, i.e., very similar to the phase ratio obtained in the 5 µm i.d. capillary (m = 0.26) for the same recipe A. This shows that the volume of the obtained layer is directly proportional to the mass of TMOS fed to the capillary: the mass fed to 10 µm i.d. capillary is 4 times larger than in the 5 µm i.d. capillary, and the volume of produced porous layer volume is also 4 times larger. This also implies that the deposited silica forms a layer with a predetermined density, independent of the capillary diameter.

The pressure-drop measurements showed an excellent linearity with the u_0-velocity (see SI, Fig. S-2). To interpret these data, it was verified how well they correlate with the well-known Hagen-Poiseuille equation,[48] given by:

$$\Delta P = \Phi_i \cdot \frac{u_i \cdot \eta \cdot L}{d^2} \qquad \text{with} \qquad \Phi_i = 32 \tag{a1}$$

Wherein Φ_i is the u_i-based flow resistance (after correction for the extra-column contributions) and wherein u_i is the average velocity in the central flow-through region (with diameter d, see Fig. 1a). Unfortunately, u_i cannot be directly measured, so that it has to be estimated from the t_0-based velocity u_0 (= L/t_0), measured using coumarin 440 (C440) in pure methanol. Doing so, the pressure-drop equation is conveniently rewritten as:

$$\Delta P = \Phi_0 \cdot \frac{u_0 \cdot \eta \cdot L}{d^2} \tag{a0}$$

In Eq. (a0), the t_0-based flow resistance Φ_0 is the only unknown, such that its value can be experimentally determined from this equation (see Table 2 for the observed values). The Φ_0 flow resistance is related to the Φ_i-resistance via the following, generally valid relation between u_i and u_0:

$$\frac{u_i}{u_0} = \frac{\Phi_0}{\Phi_i} = \frac{\varepsilon_T}{\varepsilon_e} = \frac{\varepsilon_e + (1-\varepsilon_e)\varepsilon_{pz}}{\varepsilon_e} \tag{z0}$$

wherein ε_e is the external porosity, i.e., the fraction of the original uncoated capillary remaining as the flow-through region after the application of the porous layer, related to m via $\varepsilon_e = 1/(m+1)$, and wherein ε_{pz} is the internal porosity of the porous layer after coating. To estimate the ε_{pz}-value needed in Eq. (z0), we used argon physisorption data on bulk-silica rods to determine the specific pore volume (see SI, Fig. S-3), from, which, assuming a silica density of ρ_{sil} = 2.2 g/cm^3, the internal porosity before octadecylsilylation can be obtained.[49] Subsequently assuming the mesopores have a cylindrical shape and that the C_{18}-coating has a thickness of 1 nm, the ε_{pz}-values given in Table 2 are obtained. These values lie close to the value of ε_{pz} = 0.4–0.5 that is typically obtained for silica-based mesoporous monolithic columns after octadecylsilylation.[50–53]

Subsequently using these values in Eqs. (a1) and (z0), Φ_i-value are obtained that lie very close to the theoretically expected Φ_i = 32 for all three recipes (see Table 2). Doing a reverse calculation, assuming that Φ_i = 32 (the theoretical value in the Hagen-Poiseuille equation) and calculating what ε_{pz}-value would match with the measured t_0-based flow resistance Φ_0, the values marked

with an asterisk in Table 2 are obtained. These values can be considered to agree well with the ε_{pz}-values determined via the argon physisorption measurement, especially considering the uncertainties on the different measurements on which both different values are based. From this, we dare concluding that both our pressure-drop measurements as well as our determination of the mesopore volume after coating are consistent with each other, and in agreement with theory and literature.[10,48]

It can also be observed that, regardless of the adopted measurement method, the ε_{pz}-values obtained using the different recipes lie relatively close to each other, indicating that the obtained mesoporous layer structure is always the same, independently of the amount of TMOS used in the starting solution or the final layer thickness, at least provided the same hydrothermal treatment process is applied to form the mesopores via Ostwald ripening.[47,53–55]

During the development of the recipes, it proved to be difficult to induce the phase separation needed for the "wetting transition" when further increasing the TMOS-content in the feed. For instance, it was impossible to obtain a phase separation for bulk-silica rods when increasing the TMOS content from 7.2 mL (recipe C) to 8.0 mL. This implies that, to further increase the layer thickness beyond the presently obtained values, it will be necessary to further improve preparation conditions, or to prepare a second porous layer by charging a second feed solution into an already produced PLOT capillary column, for example, as demonstrated with a pillar-array column by Detobel et al.[37] In fact, it was possible to produce a second porous layer in a very short PLOT capillary column (5 cm) (not shown), but it remains very challenging to obtain a homogenous second porous layer in long capillaries. Further improvement is necessary for charging conditions.

3.2. Chromatographic characterization and comparison with theory on *L* = 60 cm capillaries

Fig. 2 shows chromatograms of the separation of coumarins with the ODS-modified fabricated PLOT capillary columns produced by the different recipes A, B, and C. Mobile phase was 70:30% (*v*/*v*) methanol:water and linear velocity (u_0) was around 1.5 mm/s (an optimal linear velocity of OT(5)-nonporous). As can be seen, the peaks display a very good symmetry, and increasing the TMOS content provides an increase in retention factor for coumarin 480 (C480: k = 0.87–1.42), which was enhanced 35–60 times compared to that of an ODS-modified nonporous open tube (OT) capillary column (k = 0.024). In agreement with the theoretical expectations, the larger retention and layer thickness comes at the expense of some loss in column efficiency, dropping from N = 109,000 for the 300 nm layer in the PLOT(5)-A column to N = 80,000 for the 550 nm layer in the PLOT(5)-C column. In addition, the retention factor of PLOT(10)-A with an i.d. of 10 µm (k = 0.85, see SI, Fig. S-4) was similar to that of PLOT(5)-A (k = 0.87), which were produced by

the same recipe A. This can support that the volumetric phase ratio (m) between the PLOT columns was very similar regardless of different i.d., as aforementioned in the *Section 3.1*.

Fig. 3 shows chromatograms obtained at various degrees of retention achieved by varying the mobile phase composition from 60:40% (*v*/*v*) to 80:20% (*v*/*v*) and around the optimal velocity of the columns, u_0 = 0.6–0.7 mm/s. Comparing the chromatograms for the same layer thickness (vertical direction in the figure), we see an increase in *k* with increasing water fraction (following the ln(*k*) versus ϕ relationship shown in the SI in Fig. S-5). In agreement with the band broadening theory, the increase in *k* also leads to decrease in efficiency (dropping from *N* = 181,000 to *N* = 110,000 for the 300 nm layer in the PLOT(5)-A column and from *N* = 160,000 to *N* = 96,000 for the 550 nm thick layer in the PLOT(5)-C column). Comparing the chromatograms in the horizontal direction, i.e., going from a 300 nm to a 500 nm thick layer, we again observe the physically expected trend: when the layer thickness increases, the retention factor increases while the efficiency slowly decreases. Taking the 70:30% (*v*/*v*) case as an example, *k* increases from 0.87 to 1.42, while *N* drops from *N* = 150,000 to 124,000 plates when the layer increases from 300 to 550 nm (*N* = 130,000 was obtained for PLOT(5)-B with a 450 nm thickness (not shown)). Please note all cited efficiencies relate to a column length of the order of 60 cm. Plate heights (*H*) therefore vary between 3.3 to 6.3 µm (or *h* = 0.65 to 1.35 in reduced plate height units (*h* = *H*/*d*)).

Plotting the natural logarithm of the retention factors obtained at the different considered mobile phase compositions as a function of the volumetric fraction of organic modifier (ϕ), values of the solvent strength parameter *S* ($\ln k = \ln k_w - S\cdot\phi$) are obtained in the order of $S \cong 9$–10 (see SI, Fig. S-5). These values are very similar to the *S*-values typically reported in the literature on reversed-phase LC on other materials.[56]

According to the Golay-Aris theory, the plate height (*H*) in a cylindrical capillary with diameter *d* are given by:[10,57,58]

$$H = \frac{2\cdot B\cdot D_m}{u_i} + 2\cdot(C_m + C_s)\cdot\frac{d^2}{D_m}\cdot u_i \qquad \text{(a2)}$$

wherein *B,* C_m and C_s are the longitudinal diffusion and the resistance to mass transfer in the mobile zone and the porous layer, respectively given by:

$$B = \frac{1+\gamma k''}{1+k''} \qquad \text{(a3)}$$

$$C_m = \frac{1}{192} \cdot \frac{1 + 6k'' + 11k''^2}{(1 + k'')^2} \tag{a4}$$

$$C_s = \frac{k''}{(1 + k'')^2} \cdot \frac{1}{32\gamma} \cdot \left[\frac{(1 + 2\delta)^4 \ln(1 + 2\delta)}{\delta(1 + \delta)} - 12\delta(1 + \delta) - 2 \right] \tag{a5}$$

Wherein $\gamma = D_{pz}/D_m$ is the ratio of the effective diffusion in the porous layer (D_{pz}) to the liquid bulk diffusion (D_m), wherein the peculiar form of Eq. (a5) is due to the annular shape of the porous layer when it covers the wall of a cylindrical tube, and wherein k'' is the zone retention factor.[47,48,52,59,60] With u_0 measured and u_i estimated from Eq. (a0), the zone retention factor k'' and the more customarily reported phase retention factor k (based on t_0) can be calculated from the following relation to the observed retention time (corrected for system contributions):

$$t_R = t_0 \cdot (1 + k) = \frac{L}{u_i(1 + k'')} \tag{a6}$$

Fig. 4 shows all measured plate height data on the 60 cm long columns for the different considered analytes. The black symbols are the experimental data, the full lines are obtained applying Eqs. (a2)–(a5), using the measured d-, u_0-, ε_{pz}- and k-values, and the estimated ε_{pz}-values to calculate the u_i- and k''-values. The D_m-values were experimentally measured using a procedure described by Song et al., and were respectively equal to $D_m = 5.6 \times 10^{-10}$ m^2/s, $D_m = 5.1 \times 10^{-10}$ m^2/s and $D_m = 5.0 \times 10^{-10}$ m^2/s respectively for coumarin C440, C460 and C480 at 70:30% (v/v) methanol:water.[61]

With all the above known, the only fitting parameter is the effective diffusion in the porous layer (D_{pz}). Obviously, this value can be expected to be slightly different for each component, as the different components will spend a different portion of their residence time in the retained state during which they are subjected to diffusion in the stationary phase, which is known to be typically 5 to 10 times smaller than in the liquid bulk. However, the value should be the same for the different layers if the different recipes would lead to a similar pore structure. As can be noted, a very good over-all agreement between the experimental data and the Golay-Aris model is indeed obtained assuming the same D_{pz} for the three different recipes ($D_{pz} = 1.2 \times 10^{-10}$ m^2/s for C440, $D_{pz} = 1.0 \times 10^{-10}$ m^2/s for C460, $D_{pz} = 8 \times 10^{-11}$ m^2/s for C480). The order of magnitude as well as the way in which they vary with the average retention factor of the 3 different coumarins is in good agreement with literature.[62]

3.3. Chromatographic efficiencies on very long columns

Considering the excellent agreement with the Golay-Aris theory, and especially the fact that the theory can be used to predict how the band broadening varies with the layer thickness, we considered the manufacturing process to be well under control for the 60 cm format. To fully exploit the high permeability of open-tubular columns, enabling the use of very long columns, we also repeated recipe A and C to produce much longer columns (250 cm long for the recipe A column, 190 cm long for the recipe C column). The difference in length is due to the difference in the viscosity between feed solution A and C and our desire to keep same pressure (150 bar) when filling the capillaries.

A chromatogram obtained at a velocity near the optimal velocity is shown in Figs. 5a-b for the recipe A and the recipe C column respectively. Also shown are the retention factors. As can be noted these are very similar to the retention values measured on the 60 cm long columns considered in the previous section. The observed efficiencies (up to N = 600,000 for a retained, and around N = 1,000,000 plates for an unretained component for recipe A and resp. N = 350,000 and N = 550,000 for recipe C) correspond to plate heights that fit very well/exactly onto the experimental and theoretical van Deemter curves measured on(see open symbols added to Fig. 4).

In a 250 cm long column, plate counts of N = 600,000 were obtained for the 300 nm thick layer, corresponding very well to the factor of 4 increase in column length compared to the 60 cm column. In this column, a nearly unretained component provided plate counts around 1,000,000 plates in a time frame of 25 to 50 min (t_0-elution time).

As a concluding remark in the detection sensitivity, it should be noted that all peaks in the obtained chromatograms had a S/N ratio of at least 50, and on the average around 100. Knowing from the experimental Section we injected the compounds at about 3 pg each, this shows that, with the present home-build set-up we can anticipate detection limits on the order of some 100 fg with the presently employed non-optimized and home-build fluorescence detection set-up with an ordinary mercury lamp. In a next phase we will use the columns for metabolomics studies with LC/MS, where it can be expected to achieve similar detection sensitivities in the femtogram range. As such, the present research can considered to contribute to offer high efficiency and sensitivity separations to conduct biological analysis on ultra-low sample volumes where injection on very narrow i.d. columns is mandatory to prevent excessive dilution.

4. Conclusions

It is demonstrated that mesoporous silica layers with a thickness up to 550 nm can be synthesized inside open-tubular LC (OT-LC) columns with an inner diameter of 5 micrometer and a length up to 2.5 m, and that the van Deemter curves recorded in all produced columns closely follow the

Golay-Aris theory. The columns were produced using in-column sol-gel synthesis with a solution consisting of tetramethoxysilane (TMOS), urea, polyethylene glycol and acetic acid. After octadecylsilylation, chromatographic evaluation under reversed phase conditions was carried out using split-flow injection and on-column fluorescence detection using a confocal microscope. Plate counts as high as N = 150,000, N = 130,000, and N = 120,000 were obtained for respectively a 300 nm, a 450 nm and a 550 nm thick porous layer for a retained component eluting around k = 1 at the optimal flow rate in the 60 cm columns. In a 250 cm long column, plate counts of N = 600,000 were obtained for the 300 nm thick layer, corresponding very well to the factor of 4 increase in column length compared to the 60 cm column. In this column, a nearly unretained component provided plate counts around 1,000,000 plates in a time frame of 25 to 50 min (t_0-elution time).

Given the good agreement with the Golay-Aris theory observed for all produced columns, given that both the retention factors and the plate heights achieved on 60 cm long capillaries could be reproduced on 1.9 and 2.5 m long columns, and considering that mesoporous silica is still generally considered as the preferred stationary phase support in LC (and CEC), the present study could spur a renewed interest in OT-LC, especially when considering that the research in biology is targeting ever smaller and smaller samples, down to the single-cell or even sub-cellular level. In this area, a high degree of miniaturization of the separation column is mandatory.

5. Acknowledgement

T.H. gratefully acknowledges the financial support of the Research Foundation Flanders (FWO) (12C5414N). We also thank the support for scanning electron microscopy from the SURF group of the Vrije Universteit Brussel.

6. References

(1) Guiochon, G. *Anal. Che*m. **1981**, *53* (9), 1318–1325.
(2) Janssen, H. G.; Cramers, C. A. *J. Chromatogr. A*, **1990**, *505* (1), 19–35.
(3) Poppe, H. *J. Chromatogr. A*, **1997**, 778 (1–2), 3–21.
(4) Swart, R.; Kraak, J. C.; Poppe, H. *TrAC - Trends Anal. Chem.* **1997**, *16* (6), 332–342.
(5) Shen, Y.; Yang, Y. J.; Lee, M. L. *Anal. Chem.* **1997**, *69* (4), 628–635.
(6) Wu, N.; Medina, J. C.; Lee, M. L. *J. Chromatogr. A* **2000**, *892* (1–2), 3–13.
(7) Luo, Q.; Yue, G.; Valaskovic, G. A.; Gu, Y.; Wu, S.; Karger, B. L. *Anal. Chem.* **2007**, *79* (16), 6174–6181.
(8) Desmet, G.; Eeltink, S. *Anal. Chem.* **2013**, *85* (2), 543–556.
(9) Tock, P. P. H.; Duijsters, P. P. E.; Kraak, J. C.; Poppe, H. *J. Chromatogr. A* **1990**, *506* (C), 185–200.

(10) Causon, T. J.; Shellie, R. A.; Hilder, E. F.; Desmet, G.; Eeltink, S. *J. Chromatogr. A* **2011**, *1218* (46), 8388–8393.

(11) Ivanov, A. R.; Zang, L.; Karger, B. L. *Anal. Chem.* **2003**, *75* (20), 5306–5316.

(12) Shen, Y.; Moore, R. J.; Zhao, R.; Blonder, J.; Auberry, D. L.; Masselon, C.; Pasa-Tolic, L.; Hixson, K. K.; Auberry, K. J.; Smith, R. D. *Anal. Chem.* **2003**, *75* (14), 3596–3605.

(13) Luo, Q.; Shen, Y.; Hixson, K. K.; Zhao, R.; Yang, F.; Moore, R. J.; Mottaz, H. M.; Smith, R. D. *Anal. Chem.* **2005**, *77*(15), 5028–5035.

(14) Patel, K. D.; Jerkovich, A. D.; Link, J. C.; Jorgenson, J. W. *Anal. Chem.* **2004**, *76* (19), 5777–5786.

(15) Rogeberg, M.; Vehus, T.; Grutle, L.; Greibrokk, T.; Wilson, S. R.; Lundanes, E. *J. Sep. Sci.* **2013**, *36* (17), 2838–2847.

(16) Yue, G.; Luo, Q.; Zhang, J.; Wu, S.; Karger, B. L. *Anal. Chem.* **2007**, *79* (3), 938–946.

(17) Wang, D.; Hincapie, M.; Rejtar, T.; Karger, B. L., *Anal. Chem.* **2011**, *83* (6), 2029–2037.

(18) Pesek, J. J.; Matyska, M.T. *Electrophoresis* **1997**, 18 (1−2), 2228–2238.

(19) Pesek, J. J.; Matyska, M.T. *J. Chromatogr. A* **2000**, 887 (1−2), 31–41.

(20) Swart, R.; Kraak, J. C.; Poppe, H. *Chromatographia* **1995**, *40* (9–10), 587–592.

(21) Tan, Z. J.; Remcho, V. T. *Electrophoresis* **1998**, 19 (12), 2055–2060.

(22) Collins, D. A.; Nesterenko, E. P.; Brabazon, D.; Paull, B. *Chromatographia* **2013**, *76* (11–12), 581–589.

(23) Eeltink, S.; Svec, F.; Fréchet, J. M. J. *Electrophoresis* **2006**, 27 (21), 4249–4256.

(24) Abele, S.; Smejkal, P.; Yavorska, O.; Foret, F.; Macka, M. *Analyst* **2010**, *135* (3), 477–481.

(25) Nesterenko, E.; Yavorska, O.; Macka, M.; Yavorskyy, A.; Paull, B. *Anal. Methods* **2011**, *3* (3), 537–543.

(26) Collins, D. A.; Nesterenko, E. P.; Brabazon, D.; Paull, B. *Anal. Chem.* **2012**, *84* (7), 3465–3472.

(27) Knob, R.; Breadmore, M. C.; Guijt, R. M.; Petr, J.; Macka, M. *RSC Adv.* **2013**, *3* (47), 24927–24930.

(28) Kulsing, C.; Knob, R.; Macka, M.; Junor, P.; Boysen, R. I.; Hearn, M. T. W. *J. Chromatogr. A* **2014**, *1354*, 85–91.

(29) Collins, D. A.; Nesterenko, E. P.; Paull, B. *Analyst* **2014**, *139* (6), 1292–1302.

(30) Knob, R.; Kulsing, C.; Boysen, R. I.; Macka, M.; Hearn, M. T. W. *TrAC - Trends Anal. Chem.* **2015**, *67*, 16–25.

(31) Tock, P. P. H.; Boshoven, C.; Poppe, H.; Kraak, J. C.; Unger, K. K. *J. Chromatogr.* **1989**, *471* (1), 95–106.

(32) Guo, Y.; Colón, L. A. *Anal. Chem.* **1995**, *67* (15), 2511–2516.

(33) Guo, Y.; Colón, L. A. *J. Microcolumn Separations* 1995, *7* (5), 485–491.

(34) Guo, Y.; Colón, L. A. *Chromatographia* **1996**, *43* (9-10), 477–483.

(35) Kanamori, K.; Nakanishi, K.; Hirao, K.; Jinnai, H. *Colloids Surfaces A Physicochem. Eng. Asp.* **2004**, *241* (1–3), 215–224.

(36) Kanamori, K.; Nakanishi, K. *Chem. Soc. Rev.* **2011**, *40* (2), 754–770.

(37) Detobel, F.; Eghbali, H.; De Bruyne, S.; Terryn, H.; Gardeniers, H.; Desmet, G. *J. Chromatogr. A* **2009**, *1216* (44), 7360–7367.

(38) Detobel, F.; De Bruyne, S.; Vangelooven, J.; De Malsche, W.; Aerts, T.; Terryn, H.; Gardeniers, H.; Eeltink, S.; Desmet, G. *Anal. Chem.* **2010**, *82* (17), 7208–7217.

(39) De Malsche, W.; De Bruyne, S.; Op De Beeck, J.; Eeltink, S.; Detobel, F.; Gardeniers, H.; Desmet, G. *J. Sep. Sci.* **2012**, *35* (16), 2010–2017.

(40) Forster, S.; Kolmar, H.; Altmaier, S. *J. Chromatogr. A* **2012**, *1265*, 88–94.

(41) Forster, S.; Kolmar, H.; Altmaier, S. *J. Chromatogr. A* **2013**, *1283*, 110–115.

(42) Forster, S.; Kolmar, H.; Altmaier, S. *J. Chromatogr. A* **2013**, *1315*, 127–134.

(43) Hara, T.; Kobayashi, H.; Ikegami, T.; Nakanishi, K.; Tanaka, N. *Anal. Chem.* **2006**, *78* (22), 7632–7642.

(44) Hara, T.; Desmet, G.; Baron, G. V.; Minakuchi, H.; Eeltink, S. *J. Chromatogr. A* **2016**, *1442*, 42–52.

(45) Thommes, M.; Skudas, R.; Unger, K. K.; Lubda, D. *J. Chromatogr. A* **2008**, *1191* (1-2), 57–66.

(46) Thommes, M. *Chemie-Ingenieur-Technik* **2010**, *82* (7), 1059–1073.

(47) Unger, K. K.; Tanaka, N.; Machtejevas, E. *Monolithic Silicas in Separation Science: Concepts, Syntheses, Characterization, Modeling and Applications*; Wiley-VCH Verlag GmbH&Co.KGaA: Weinheim, 2011.

(48) Giddings, C. *Dynamics of Chromatography: Principles and Theory*; Dekker, M., Ed.; CRC Press: New York, 1965.

(49) Neue, D. U. *HPLC Columns: Theory, Thechnology, and Practice*; Wiley-VCH: New York, 1997.

(50) Minakuchi, H.; Nakanishi, K.; Soga, N.; Ishizuka, N.; Tanaka, N. *J. Chromatogr. A* **1997**, *762* (1–2), 135–146.

(51) Minakuchi, H.; Nakanishi, K.; Soga, N.; Ishizuka, N.; Tanaka, N. *J. Chromatogr. A* **1998**, *797* (1–2), 121–131.

(52) Gritti, F.; Guiochon, G. *J. Chromatogr. A* **2012**, *1227*, 82–95.

(53) Hara T., *Study on Preparation and Characterization of Monolithic Silica Capillary Columns for High Separation Efficiency in High Performance Liquid Chromatography*, PhD thesis in Justus-Liebig-Universität Giessen (online available), 2013.

(54) Nakanishi, K. *J. Porous Mater.* **1997**, *4* (2), 67–112.

(55) Galarneau, A.; Iapichella, J.; Brunel, D.; Fajula, F.; Bayram-Hahn, Z.; Unger, K.; Puy, G.; Demesmay, C.; Rocca, J.-L. *J. Sep. Sci.* **2006**, *29* (6), 844–855.

(56) Snyder, L. R; Dolan, J. W, *High-Performance Gradient Elution: The Practical Application of the Linear-Solvent-Strength Model*; John Wiley & Sons, Inc.: New Jersey, 2007.

(57) Schisla, D.; Carr, P. W. *Chromatographia* **1990**, *29* (11), 606–608.

(58) Desmet, G.; Baron, G. V. *J. Chromatogr. A* **2000**, *867* (1–2), 23–43.

(59) Knox, J. H. *J. Chromatogr. Sci.* **1977**, *15*, 352–364.

(60) Desmet, G.; Broeckhoven, K. *Anal. Chem.* **2008**, *80* (21), 8076–8088.

(61) Song, H.; Vanderheyden, Y.; Adams, E.; Desmet, G.; Cabooter, D. *J. Chromatogr. A* **2016**, *1455*, 102–112.

(62) Liekens, A.; Denayer, J.; Desmet, G. *J. Chromatogr. A* **2011**, *1218* (28), 4406–4416.

Figure captions

Figure 1. Scanning electron micrographs of **(a)** PLOT(5)-A, 5 µm i.d. capillary with recipe A (5.0 mL TMOS), **(b)** PLOT(5)-B, 5 µm i.d. capillary with recipe B (6.4 mL TMOS), and **(c)** PLOT(5)-C, 5 µm i.d. capillary with recipe C (7.2 mL TMOS). The measurements were carried out at 10000-fold magnification and the scale bars correspond to 500 nm.

Figure 2. Chromatograms obtained for coumarins C440, C460 and C480 with ODS-modified PLOT capillary columns. Column: **(a)** OT(5)-nonporous, **(b)** PLOT(5)-A, **(c)** PLOT(5)-B, and **(d)** PLOT(5)-C. Mobile phase: 70:30% (*v*/*v*) methanol:water. Measurement temperature: 25 °C. Effective length and total length are shown for all the columns. Retention factor (*k*), theoretical plate number (*N*), and plate height (*H*) observed for coumarin 480 are shown.

Figure 3. Chromatograms obtained for coumarins C440, C460 and C480 in different mobile phase compositions. Columns: **(a)** PLOT(5)-A and **(b)** PLOT(5)-C. 60:40%–80:20% (*v*/*v*) methanol:water mixtures were used as mobile phase. Measurement temperature: 25 °C. Retention factor (*k*), theoretical plate number (*N*), and plate height (*H*) observed for coumarin 480 are shown. Effective length and total length for the columns are same as shown in Figure 2.

Figure 4. Plots of plate height against reduced mobile phase velocity with ODS-modified PLOT capillary columns. Solute: **(a)** Coumarin 440, **(b)** coumarin 460, and **(c)** coumarin 480. Symbol: PLOT(5)-A (●), PLOT(5)-C (▲), and PLOT-C (■). The symbol sizes correspond to the min-max error bars (n = 3). Mobile phase: 70:30% (*v*/*v*) methanol:water. Measurement temperature: 25 °C. Open symbols express the data obtained with the longer PLOT(5)-A and PLOT(5)-C columns (see Figure 5).

Figure 5. Chromatograms obtained for coumarins C440, C460 and C480 with ODS-modified long PLOT capillary columns: **(a)** PLOT(5)-A-long **(b)** PLOT(5)-C-long. Measurement conditions are same as shown in Figure 2. Effective length and total length are shown for the columns. Retention factor (*k*), theoretical plate number (*N*), and plate height (*H*) observed for all the coumarins are shown.

Tables

Table 1. Preparation conditions for porous layered open tube capillary columns[a]

Column	TMOS (mL)	PEG (g)	Urea (g)	0.01M aqueous acetic acid solution (mL)
PLOT(5)-A PLOT(10)-A	5.0	0.430	0.900	10
PLOT(5)-B	6.4	0.860	0.900	10
PLOT(5)-C	7.2	0.730	0.900	10

[a] Detailed information on preparation processes is shown in the "*Experimental*" section.

Table 2. Results of flow-measurement of porous layered open tube capillary columns[i]

Parameters	PLOT(5)-A	PLOT(5)-B	PLOT(5)-C
d_{cap} (μm)[a]	5.69	5.71	5.71
δ (nm)[a]	306	478	563
d (μm)[a]	5.08	4.76	4.59
ε_e[b]	0.80	0.69	0.65
m[c]	0.26	0.44	0.55
Φ_0[d]	36.3	39.6	39.4
ε_{pz}[e]	0.41	0.47	0.47
ε_T[f]	0.88	0.84	0.81
Φ_i[g]	32.5	33.1	31.6
ε_{pz*}[h]	0.52	0.54	0.42

[a] All the values were calculated using SEM images (see "*Experimental*" section).

[b] External column porosity(ε_e) was determined by the equation "$\varepsilon_e = (d_{cap}-\delta)^2/d_{cap}{}^2$".

[c] Volumetric phase ratio (m) was calculated according to Eq. (1).

[d] t_0-Based flow resistance (Φ_0) was assessed by Eq. (a0).

[e] Silica Layer porosity (ε_{pz}) was estimated by using the argon physisorption data on the corresponding bulk-silica rods.

[f] Total column porosity (ε_T) was calculated by Eq. (z0) and the silica layer porosity (ε_{pz}) was assumed as $\varepsilon_{pz} = 0.45$ for the calculation.

[g] u_i-Based flow resistance (Φ_i) was obtained by Eq.(a1).

[h] Silica Layer porosity (ε_{pz*}) was estimated by applying $\Phi_i = 32$ (constant).

[i] Flow measurements were conducted with coumarin 440 in 100:0% (v/v) methanol:water, resulting in relative standard values (RSDs) < 0.17% regarding t_0-based flow resistance (Φ_0) when it was calculated from 3 times-measurements under a constant column pressure drop (ΔP).

Fig. 1

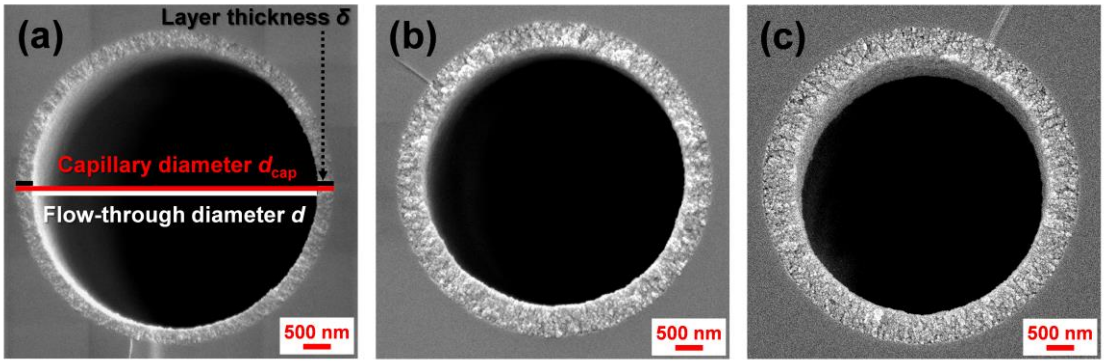
(a)
Layer thickness δ
Capillary diameter d_{cap}
Flow-through diameter d
500 nm
(b)
500 nm
(c)
500 nm

Fig. 2

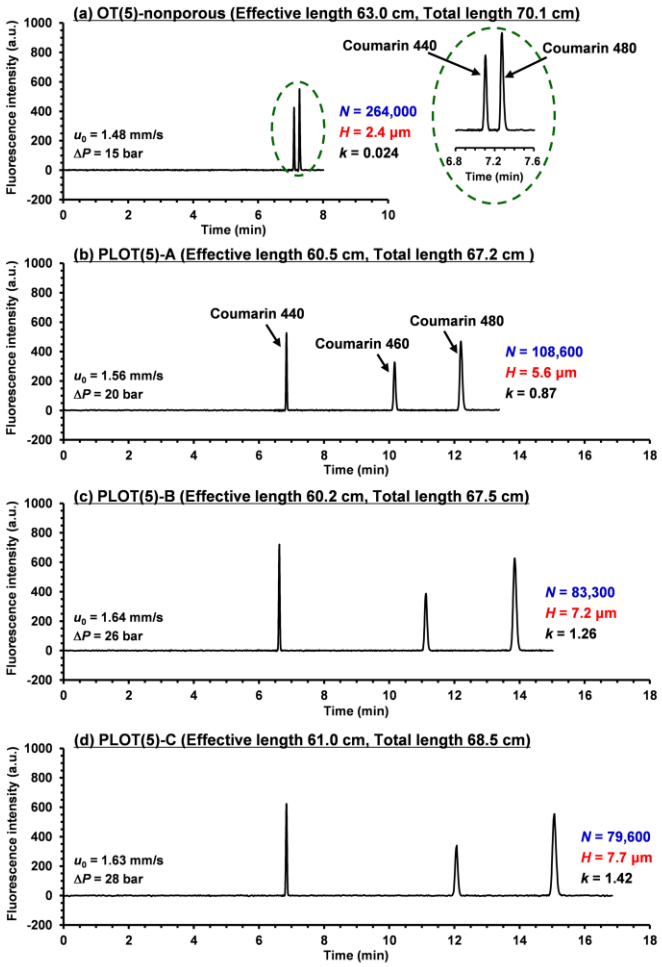
(a) OT(5)-nonporous (Effective length 63.0 cm, Total length 70.1 cm)
Coumarin 440
Coumarin 480
N = 264,000
H = 2.4 μm
k = 0.024
u0 = 1.48 mm/s
ΔP = 15 bar
Fluorescence intensity (a.u.)
Time (min)
(b) PLOT(5)-A (Effective length 60.5 cm, Total length 67.2 cm)
Coumarin 440
Coumarin 460
Coumarin 480
N = 108,600
H = 5.6 μm
k = 0.87
u0 = 1.56 mm/s
ΔP = 20 bar
(c) PLOT(5)-B (Effective length 60.2 cm, Total length 67.5 cm)
N = 83,300
H = 7.2 μm
k = 1.26
u0 = 1.64 mm/s
ΔP = 26 bar
(d) PLOT(5)-C (Effective length 61.0 cm, Total length 68.5 cm)
N = 79,600
H = 7.7 μm
k = 1.42
u0 = 1.63 mm/s
ΔP = 28 bar

Fig. 3

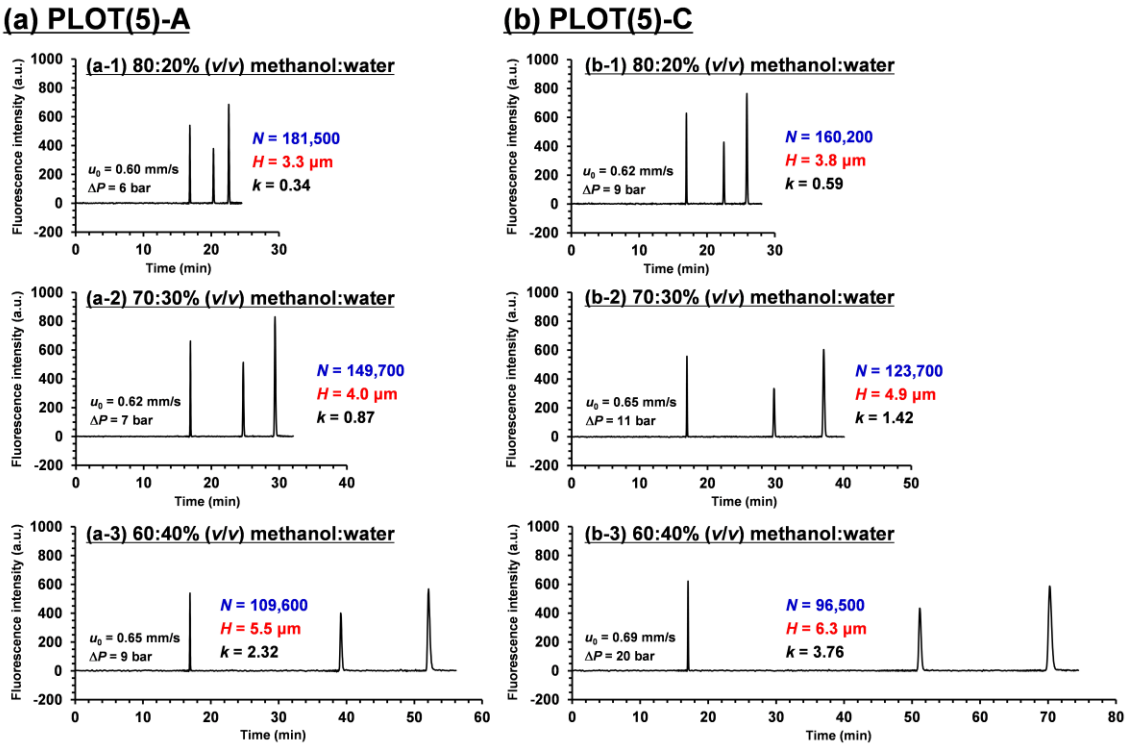
(a) PLOT(5)-A
(a-1) 80:20% (v/v) methanol:water
N = 181,500
H = 3.3 μm
k = 0.34
u0 = 0.60 mm/s
ΔP = 6 bar
(a-2) 70:30% (v/v) methanol:water
N = 149,700
H = 4.0 μm
k = 0.87
u0 = 0.62 mm/s
ΔP = 7 bar
(a-3) 60:40% (v/v) methanol:water
N = 109,600
H = 5.5 μm
k = 2.32
u0 = 0.65 mm/s
ΔP = 9 bar
(b) PLOT(5)-C
(b-1) 80:20% (v/v) methanol:water
N = 160,200
H = 3.8 μm
k = 0.59
u0 = 0.62 mm/s
ΔP = 9 bar
(b-2) 70:30% (v/v) methanol:water
N = 123,700
H = 4.9 μm
k = 1.42
u0 = 0.65 mm/s
ΔP = 11 bar
(b-3) 60:40% (v/v) methanol:water
N = 96,500
H = 6.3 μm
k = 3.76
u0 = 0.69 mm/s
ΔP = 20 bar
Fluorescence intensity (a.u.)
Time (min)

Fig. 4

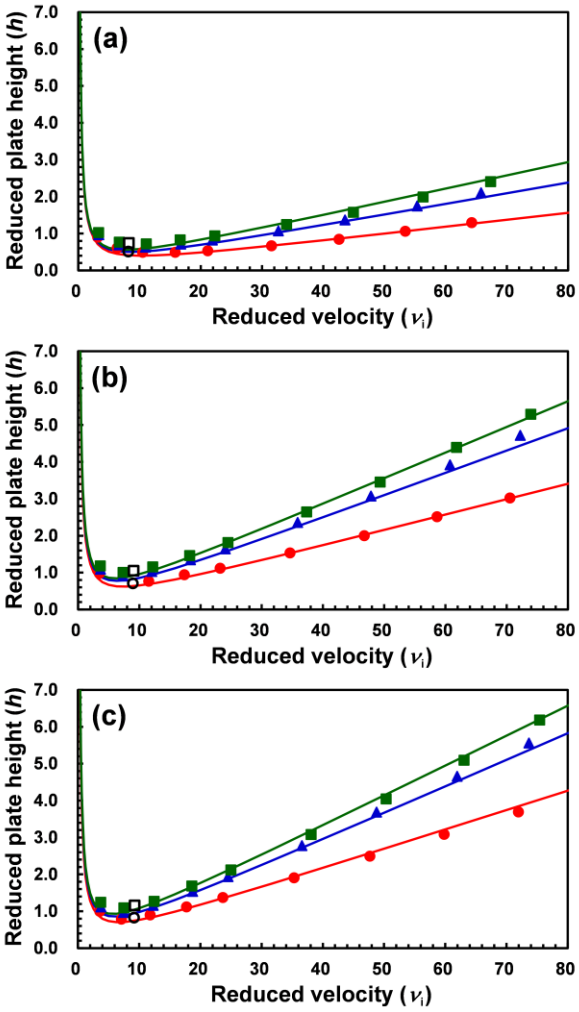
(a)
(b)
(c)
Reduced plate height (h)
Reduced velocity (ν_i)
0.0
1.0
2.0
3.0
4.0
5.0
6.0
7.0
0
10
20
30
40
50
60
70
80

Fig. 5

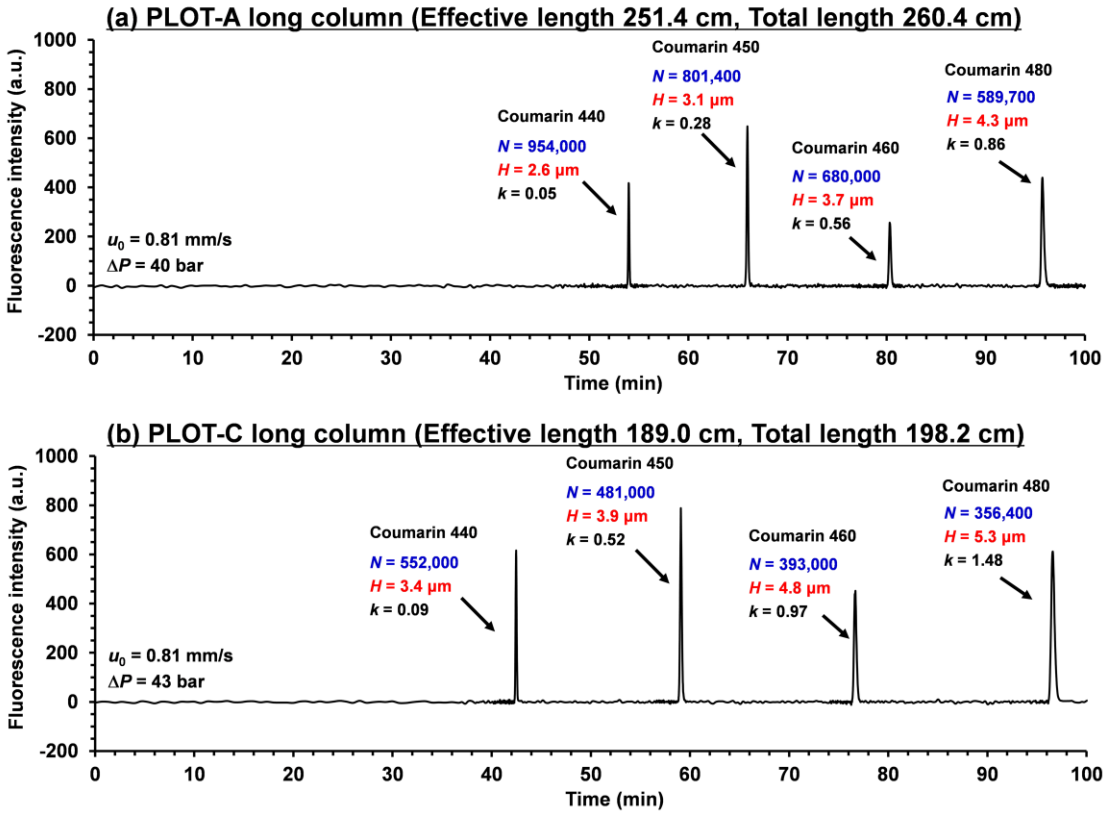
(a) PLOT-A long column (Effective length 251.4 cm, Total length 260.4 cm)
Fluorescence intensity (a.u.)
Time (min)
Coumarin 440
N = 954,000
H = 2.6 μm
k = 0.05
Coumarin 450
N = 801,400
H = 3.1 μm
k = 0.28
Coumarin 460
N = 680,000
H = 3.7 μm
k = 0.56
Coumarin 480
N = 589,700
H = 4.3 μm
k = 0.86
u0 = 0.81 mm/s
ΔP = 40 bar
(b) PLOT-C long column (Effective length 189.0 cm, Total length 198.2 cm)
Fluorescence intensity (a.u.)
Time (min)
Coumarin 440
N = 552,000
H = 3.4 μm
k = 0.09
Coumarin 450
N = 481,000
H = 3.9 μm
k = 0.52
Coumarin 460
N = 393,000
H = 4.8 μm
k = 0.97
Coumarin 480
N = 356,400
H = 5.3 μm
k = 1.48
u0 = 0.81 mm/s
ΔP = 43 bar

Table of Content (TOC)

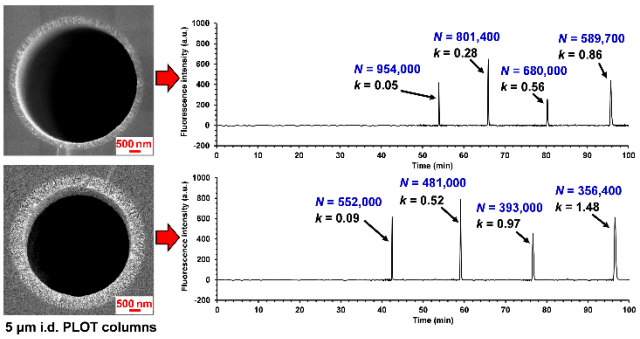

5 µm i.d. PLOT columns